JOURNAL OF VIROLOGY, Oct. 2007, p. 11226–11235 Vol. 81, No. 20
0022-538X/07/$08.00+0 doi:10.1128/JVI.00431-07

Distinct Intracellular Trafficking of Equine Infectious Anemia Virus and Human Immunodeficiency Virus Type 1 Gag during Viral Assembly and Budding Revealed by Bimolecular Fluorescence Complementation Assays▽

Jing Jin,[1,4] Timothy Sturgeon,[1] Chaoping Chen,[5] Simon C. Watkins,[3] Ora A. Weisz,[2,3] and Ronald C. Montelaro[1,4]*

Department of Molecular Genetics and Biochemistry,[1] Department of Medicine, Renal-Electrolyte Division,[2] and Department of Cell Biology and Physiology,[3] School of Medicine, University of Pittsburgh, Pittsburgh, Pennsylvania 15261; Department of Infectious Disease and Microbiology, Graduate School of Public Health, University of Pittsburgh, Pittsburgh, Pennsylvania 15261[4]; and Department of Biochemistry and Molecular Biology, Colorado State University, Fort Collins, Colorado 80523[5]

Received 28 February 2007/Accepted 2 August 2007

Retroviral Gag polyproteins are necessary and sufficient for virus budding. Numerous studies of human immunodeficiency virus type 1 (HIV-1) Gag assembly and budding mechanisms have been reported, but relatively little is known about these fundamental pathways among animal lentiviruses. While there may be a general assumption that lentiviruses share common assembly mechanisms, studies of equine infectious anemia virus (EIAV) have indicated alternative cellular pathways and cofactors employed among lentiviruses for assembly and budding. In the current study, we used bimolecular fluorescence complementation to characterize and compare assembly sites and budding efficiencies of EIAV and HIV-1 Gag in both human and rodent cells. The results of these studies demonstrated that replacing the natural RNA nuclear export element (Rev-response element [RRE]) used by HIV-1 and EIAV with the hepatitis B virus posttranscriptional regulatory element (PRE) altered HIV-1, but not EIAV, Gag assembly sites and budding efficiency in human cells. Consistent with this novel observation, different assembly sites were revealed in human cells for Rev-dependent EIAV and HIV-1 Gag polyproteins. In rodent cells, Rev-dependent HIV-1 Gag assembly and budding were blocked, but changing RRE to PRE rescued HIV-1 Gag assembly and budding. In contrast, EIAV Gag polyproteins synthesized from mRNA exported via either Rev-dependent or PRE-dependent mechanisms were able to assemble and bud efficiently in rodent cells. Taken together, our results suggest that lentivirus assembly and budding are regulated by the RNA nuclear export pathway and that alternative cellular pathways can be adapted for lentiviral Gag assembly and budding.

Retrovirus assembly and budding is a highly concerted process mediated by largely undefined spatially and temporally regulated interactions between viral proteins and cellular factors. During the viral assembly process, thousands of copies of viral structural polyproteins multimerize via noncovalent low-affinity interactions to form virus particles. Expression of retroviral Gag polyprotein is generally sufficient for the assembly and release of noninfectious virus-like particles (VLPs). The Gag polyprotein consists of matrix, capsid, nucleocapsid, and late (L) domains and is cleaved into the distinct structural proteins upon virus maturation (10, 29). These Gag domains orchestrate the major steps in virus assembly and budding (reviewed in references 10 and 27). Recent studies have revealed that retrovirus L domains recruit cellular factors that normally function in the invagination of late endosomes/multivesicular bodies (MVBs). However, where and how Gag assembly occurs is still controversial. Among the retroviruses, trafficking and assembly of HIV-1 Gag has been the most extensively studied. It is well established that HIV-1 Gag buds from the plasma membrane of T lymphocytes and of some epithelial cell lines such as HeLa and Cos cells (10, 17, 29, 31–33, 35). In contrast, in macrophages and dendritic cells, the major histocompatibility complex class II compartment or MVB is apparently the site of HIV-1 Gag accumulation and particle production (2, 29, 31, 32, 40, 42). In additions, various studies also indicate that HIV-1 Gag may also target to MVBs in other cell types (33, 35, 45). The critical cellular and viral determinants that mediate HIV-1 Gag targeting are not known; however, a recent report suggests that HIV-1 Gag assembly is regulated as early as nuclear export of its encoding mRNA (48, 49).

Retroviral Gag polyproteins are synthesized from an unspliced full-length viral genomic mRNA that requires specific regulatory factors for nuclear export. Lentiviruses contain a *cis*-acting RNA element known as the Rev-response element (RRE) that binds to a viral *trans*-acting protein (Rev). Rev binds to the cellular Crm1 protein which in turn binds to Ran, a small GTPase that shuttles between the nucleus and the cytoplasm. At least some simple retroviruses, such as Mason-Pfizer monkey virus, contain *cis*-acting RNA export elements (constitutive transport elements [CTE]) that do not require viral *trans*-acting factors and that function by interacting di-

* Corresponding author. Mailing address: Department of Molecular Genetics and Biochemistry, University of Pittsburgh School of Medicine, W1144 Biomedical Science Tower, Pittsburgh, PA 15261. Phone: (412) 648-8869. Fax: (412) 383-8859. E-mail: rmont@pitt.edu.

▽ Published ahead of print on 8 August 2007.

rectly with cellular export factors NXF1/NXT (48). Swanson et al. (49) recently demonstrated in murine cells, which are notable for their inability to support HIV-1 assembly and budding (1, 26, 49), that altering the RNA nuclear export element used by HIV-1 *gag-pol* mRNA from the RRE to the CTE resulted in efficient trafficking and assembly of Gag at cellular membranes. These results support the model that RNA export pathway selection during Gag expression and assembly can modulate the cytosolic fate or function of the viral core polyproteins. This model is also supported by earlier reports that the observed deficiency of assembly of avian leukosis virus in mammalian cells could be overcome by replacement of the avian leukosis virus CTE-mediated mRNA nuclear export pathway with the HIV-1 Rev-RRE-mediated mRNA nuclear export pathway (30, 34).

Equine infectious anemia virus (EIAV), an ungulate lentivirus, has been used to examine the mechanisms of animal lentivirus assembly and budding, and the results of these studies have provided novel insights into the molecular and cellular biology of these fundamental lentiviral processes. Unlike with other retroviruses, EIAV Gag budding seems to be ubiquitin independent (38, 44), and its unique YPDL L-domain recruits Alix/AIP1 as the budding partner (7, 27, 47, 52). Little is known about the trafficking pathway and assembly site(s) of EIAV Gag. Like other lentiviruses, EIAV Gag is expressed from full-length genomic mRNA that is exported from the nucleus with the aid of the viral accessory protein Rev. Whether or not EIAV Gag assembly and budding are regulated by nuclear export of its encoding mRNA is unknown. We previously generated an EIAV Gag expression vector by attaching the hepatitis B virus posttranscriptional regulatory element (PRE) to the *gag* gene (38). This PRE-based vector has been used successfully in various applications related to retrovirus assembly and budding (6, 38, 44), and results obtained by using PRE-based EIAV Gag expression vector were similar to those with Rev-dependent EIAV proviral constructs (38). Although the detailed mechanisms of PRE-mediated RNA nuclear export remain to be defined, the PRE appears to utilize an export pathway different from that of HIV-1 and EIAV Rev and of the Mason-Pfizer monkey virus CTE (37, 54), thus providing a novel system in which to examine the effects of nuclear export pathways on EIAV Gag assembly and budding in comparison to HIV-1.

In this study, we used the bimolecular fluorescence complementation (BiFC) assay to study both Rev-dependent and PRE-dependent (hereafter termed Rev-independent) EIAV and HIV-1 Gag assembly and budding. The BiFC technique offers a powerful new tool to detect protein-protein interactions with high levels of specificity and sensitivity (19, 20, 22). The BiFC assay has been used to demonstrate coassembly of HIV-1 and HIV-2 Gag (3), and we recently used the BiFC assay to demonstrate close and specific interactions between EIAV Gag and actin (6). In this assay, a fluorescence protein gene is divided into N-terminal and C-terminal segments. Separately, the encoded fragments are unable to fluoresce; however, coexpression of interacting proteins individually fused to these fragments generates detectable fluorescence signal when the two fluorescent protein fragments are placed in close proximity (less than 15 nm). In the current studies, we utilized the BiFC assay to characterize and compare assembly of EIAV and HIV-1 Gag in human and rodent cell lines and to define the influence of variant mRNA nuclear export pathways on Gag assembly and budding by the two lentiviruses.

MATERIALS AND METHODS

DNA mutagenesis. Overlapping PCR was used to construct Gag mutations and fusion proteins (5). For BiFC assays, sequences encoding the amino (residues 1 to 173, VN) or carboxyl (residues 155 to 238, VC) fragments of Venus fluorescence protein (template generously provided by Atsushi Miyawaki, RIKEN Brain Science Institute, Saitama, Japan) were fused to the C terminus of EIAV or HIV-1 Gag via a six-alanine linker. Detailed sequence information for each construct is available upon request. To make hemagglutinin (HA) epitope-tagged Gag polyproteins, the YPYDVPDYA epitope from influenza virus HA protein was inserted into the C terminus of p9 or p6 protein. All plasmids were isolated using a QIAGEN Midiprep kit (QIAGEN, Valencia, CA), and the specific mutations were confirmed by DNA sequencing.

Cell culture and transfection. HeLa SS6 and 293T cells were cultured in Dulbecco's minimal essential medium (DMEM) supplemented with 10% fetal bovine serum. NIH 3T3 cells were maintained in DMEM supplemented with 10% newborn calf serum. Equine dermal (ED) cells were cultured in MEM supplemented with 10% fetal bovine serum. Cells were transfected using Lipofectamine 2000 (Invitrogen, Calsbad, CA) following the procedures outlined by the manufacturer.

Gag protein expression assays. At 48 h posttransfection, cells were harvested and lysed in lysis buffer (25 mM Tris-HCl, pH 8.0, 150 mM NaCl, 1% deoxycholic acid, 1% Triton X-100, 1× protease inhibitor cocktail) and centrifuged at 20,800 × *g* for 5 min to remove cell nuclei. VLPs released into the culture medium were pelleted by centrifugation (20,800 × *g* for 3 h at 4°C) and resuspended in phosphate-buffered saline (PBS). HA-Gag contained in cell lysates and VLPs was analyzed by Western blotting using rat anti-HA antibody epitope (Roche Applied Science, Indianapolis, IN) and HRP-conjugated goat anti-rat immunoglobulin G (IgG) (Zymed, San Francisco, CA).

Confocal microscopy. Transfected cells grown on coverslips were fixed and permeabilized with 2% paraformaldehyde and 0.1% Triton X-100 in PBS. VLPs were adsorbed onto coverslips by overnight incubation at 4°C in the presence of 16 μg/ml Polybrene and then fixed with 2% paraformaldehyde. Images were captured using a Leica TCS-SL microscope and processed with Metamorph software.

Flow cytometry analysis. HeLa SS6 and NIH 3T3 cells grown on six-well plates were transfected with selected BiFC construct pairs. Cells were detached with PBS containing 2.5 mM EDTA and resuspended in PBS at 16 h posttransfection for HeLa SS6 cells and at 48 h posttransfection for NIH 3T3 cells. For HA staining (see Fig. 3 and 4), cells were washed three times with PBS containing 5% fetal bovine serum (wash buffer) and fixed in 1% paraformaldehyde for 1 h, followed by permeabilization with PBS containing 5% fetal calf serum and 0.5% saponin. Mouse anti-HA epitope antibody (Santa Cruz Biotechnology, Santa Cruz, CA) and Cy5-conjugated goat anti-mouse IgG (Jackson ImmunoResearch Laboratory, West Grove, PA) were used to stain HeLa SS6 cells, while rat anti-HA epitope antibody and Cy5-conjugated goat anti-rat IgG (Zymed, San Francisco, CA) were used to stain NIH 3T3 cells. A minimum of 30,000 gated live events were acquired on a FACSCalibur (Becton Dickinson, San Jose, CA) flow cytometer and analyzed with FlowJo batch analysis software (Treestar, San Carlos, CA) for both yellow fluorescence and HA staining (see Fig. 3 and 4).

RESULTS

Expression of Rev-dependent and Rev-independent EIAV and HIV-1 Gag-BiFC constructs. Using the optimized amino (VN)- and carboxy (VC)-terminal fragments of Venus fluorescence protein (46), we first generated a panel of Gag-BiFC constructs (shown in Fig. 1A) for EIAV and HIV-1 Gag. The EIAV *gag* gene in pPRE-Gag (38) was replaced with VN- or VC-tagged EIAV or HIV-1 Gag genes to generate Rev-independent expression vectors. Rev-dependent EIAV and HIV-1 Gag-BiFC constructs were generated based on EIAV and HIV-1 proviral constructs pCMVuk (38) and pNL4-3/KFS (15), respectively. The U3 regions of both EIAV and HIV-1 proviral constructs were replaced by a cytomegalovirus pro-

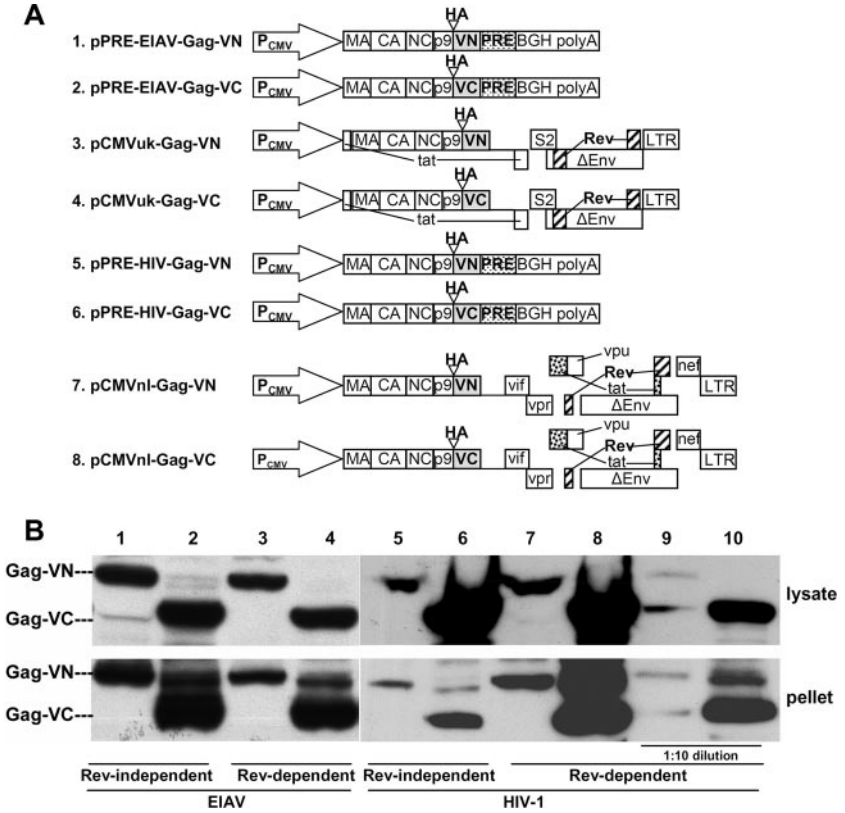

FIG. 1. Expression and budding of Rev-dependent and Rev-independent Gag-BiFC constructs in 293T cells. (A) Schematic diagram of plasmids expressing EIAV and HIV-1 Gag-BiFC fusion proteins in either Rev-dependent or Rev-independent manner. An HA epitope indicated by an arrowhead was inserted at the C terminus of p9 or p6 protein. (B) Expression and budding of the constructs depicted in panel A in transfected 293T cells, as described in Materials and Methods. Lanes 1 to 8 in this panel correspond directly to constructs 1 to 8 in panel A. Lanes 9 and 10 were loaded with 1:10 diluted samples loaded in lanes 7 and 8, respectively. At 48 h posttransfection, cell lysates (upper panel) and VLPs (lower panel) were analyzed by immunoblotting using HA antibody.

moter to obtain similar transcriptional levels from both Rev-dependent and Rev-independent vectors. Envelope glycoprotein expression was eliminated by introduction of a premature stop codon or frameshift, and *pol* genes were deleted to facilitate cloning. The inserted HA epitope provides a common tag to directly compare the expression of the various fusion constructs. We first examined the relative efficiency of protein expression and VLP budding by the panel of Gag constructs (Fig. 1B) in 293T cells transfected with the individual vectors. At 48 h posttransfection, cell lysates and supernatant VLPs were subjected to sodium dodecyl sulfate-polyacrylamide gel electrophoresis and Western blot analysis with HA antibody. The immunoblot data indicated that all of the Gag-BiFC fusion proteins for EIAV and HIV-1 were expressed and released in VLPs. However, differences in the influence of mRNA nuclear export pathways on Gag budding efficiency were observed between EIAV and HIV-1. Expression and budding of EIAV Gag-BiFC constructs were similar when expressed in 293T cells from plasmids encoding either Rev-independent (Fig. 1, lanes 1 and 2) or Rev-dependent (Fig. 1, lanes 3 and 4) Gag constructs. In contrast, the budding efficiency of HIV-1 Gag-BiFC fusion proteins expressed from Rev-independent vectors was roughly 10-fold lower than that of Rev-dependent Gag fusion proteins (compare VLPs in lanes 5 and 6 with lanes 7 and 8 and their 10-fold dilutions shown in lanes 9 and 10 of Fig. 1), although the amounts of proteins produced in the transfected cells were highly comparable under both conditions (compare lysates in lanes 5 and 6 with lanes 7 and 8 of Fig. 1).

Demonstration of EIAV Gag assembly by BiFC assay. We next used the BiFC assay to examine EIAV Gag assembly by confocal microscopy in EIAV-permissive ED cells (Fig. 2, panels a to c) and in HeLa cells (Fig. 2, panels d to f). Both ED (Fig. 2, panel b) and HeLa (Fig. 2, panel e) cells expressing Rev-independent EIAV-Gag-yellow fluorescent protein (YFP) displayed intracellular punctate YFP signals. In ED (Fig. 2, panel a) and HeLa cells (Fig. 2, panel d) transfected with the Rev-independent EIAV Gag-VN/Gag-VC pair, intracellular YFP fluorescence was observed, indicating the interaction of Gag monomers with one another during VLP assembly. This EIAV Gag-Gag-BiFC distribution pattern resembled the Rev-independent EIAV-Gag-YFP intracellular distribution pattern, suggesting Gag-Gag-BiFC signals correctly represent intracellular Gag assembly. We previously used the BiFC assay and demonstrated a lack of detectable interaction between EIAV Gag and tubulin in transfected cells (6), so the EIAV Gag-VN/VC-tubulin pair was employed in the current study as a negative control for the current BiFC assays. No positive BiFC signal was observed in ED (Fig. 2, panel c) or HeLa cells (Fig. 2, panel f) transfected with the Gag-VN/VC-tubulin con-

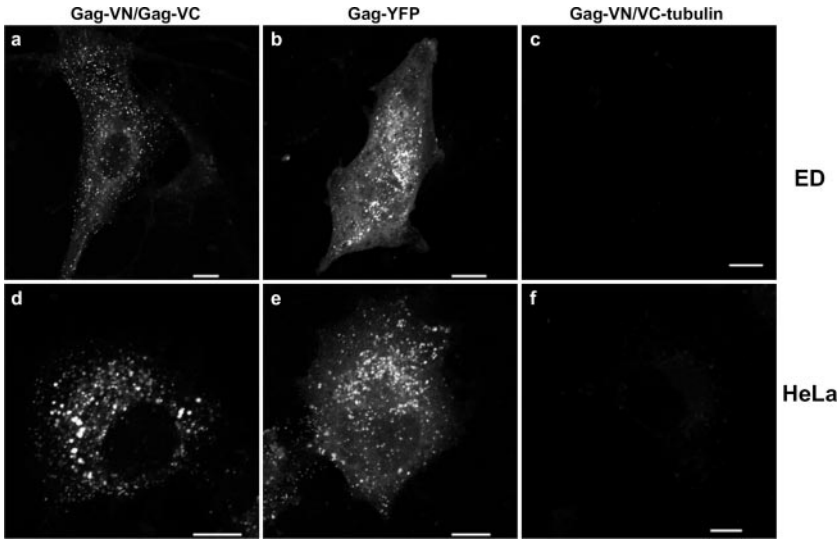

FIG. 2. Demonstration of EIAV Gag assembly by the BiFC assay. ED (panels a to c) and HeLa (panels d to f) cells grown on glass coverslips were transfected with pPRE-EIAV-Gag-VN and pPRE-EIAV-Gag-VC (panels a and d), pPRE-EIAV-Gag-YFP (panels b and e), and pPRE-EIAV-Gag-VN and pCMV-VC-tubulin (panels c and f) plasmid using Lipofectamine 2000. At 24 h posttransfection, cells were fixed and imaged with a Leica TCS-SL confocal microscope. Bar, 10 μm.

trol pair, confirming the specificity of the observed Gag-Gag interactions.

Comparison of Rev-dependent and Rev-independent EIAV and HIV-1 Gag assembly. We next used the BiFC assay to characterize and compare EIAV and HIV-1 Gag assembly in human (Fig. 3) and rodent (Fig. 4) cells by confocal microscopic and flow cytometric analysis of cells transfected with the indicated Gag-VN/Gag-VC pairs. Due to the lower expression level of HIV-Gag-VN compared to HIV-Gag-VC (Fig. 1B), a 5:2 mass ratio of HIV-1 Gag-VN expression vector to HIV-1 Gag-VC expression vector was used for HIV-1 Gag-VN/Gag-VC cotransfection to optimize the BiFC signal. Four micrograms of total DNA was used to transfect one well of cells grown in six-well plates for both confocal microscopy and flow cytometry analyses.

Both Rev-dependent and Rev-independent EIAV Gag polyproteins assembled efficiently in HeLa and 293T cells (Fig. 3A, panels a, b, e, and f), and expression of EIAV Gag-VN/Gag-VC pairs resulted in a bright punctate fluorescent signal distributed throughout the cytoplasm and along the cell surface, with some concentration in the juxtanuclear region. In contrast, we observed a dramatic difference between the BiFC patterns in cells expressing Rev-independent compared to Rev-dependent HIV-1 Gag constructs. Cotransfection of Rev-independent HIV-1 Gag-VN/Gag-VC constructs into human cells resulted in a weak BiFC signal overall, consisting of a few intracellular puncta over a diffuse cytoplasmic background (Fig. 3A, panels c and g). In marked contrast, human cells expressing Rev-dependent HIV-1 Gag-VN/Gag-VC constructs displayed bright cell surface BiFC signal (Fig. 3A, panels d and h). Examining cells transfected with 4 μg or 0.4 μg of DNA after overnight transfection or as early as 9 h posttransfection yielded similar results (data not shown). These results indicate that the mRNA nuclear export pathways can alter HIV-1 Gag assembly sites, as reported previously (49), and that alternative assembly/budding sites are apparently utilized by EIAV and HIV-1 Gag.

To quantify the assembly efficiency of Rev-dependent and Rev-independent EIAV and HIV-1 Gag, HeLa cells expressing the indicated BiFC pairs were analyzed by flow cytometry (Fig. 3B). To normalize differences in transfection efficiency and Gag expression levels, fixed and permeabilized cells were stained with mouse HA antibody followed by Cy5-conjugated secondary antibody. The ratio of HA and BiFC double-positive populations to the total HA-positive population was used to calculate assembly efficiency. Cells transfected with an HA-tagged VN-actin/VC-actin pair were used as a positive control, as described previously (6). In VN-actin/VC-actin-cotransfected human cells, almost 44% of HA-positive cells exhibited positive BiFC signal (Fig. 3B, panel e), while none of the HA-positive cells displayed yellow fluorescence in mock-transfected control (Fig. 3B, panel f). A similar assembly efficiency was observed for Rev-independent (Fig. 3B, panel a) or Rev-dependent (Fig. 3B, panel b) EIAV Gag (13.3% and 14.6%, respectively). In contrast, lower assembly efficiency (0.5%) was observed for Rev-independent HIV-1 Gag (Fig. 3B, panel c) compared with the assembly efficiency (2.4%) for Rev-dependent HIV-1 Gag (Fig. 3B, panel d).

As observed in human cells, expression of both Rev-independent (Fig. 4A, panel a) and Rev-dependent (Fig. 4A, panel b) EIAV Gag-VN/Gag-VC pairs in mouse-derived NIH 3T3 cells resulted in an intracellular punctate BiFC pattern. In contrast, a weak but distinct BiFC signal was observed when Rev-independent HIV-1 Gag-VN/Gag-VC constructs were expressed in NIH 3T3 cells (Fig. 4A, panel c), while only background signal could be detected in NIH 3T3 cells expressing the Rev-dependent HIV-1 Gag-VN/Gag-VC pair (Fig. 4A, panel d). These qualitative microscopy results were further supported by quantitative flow cytometry data (Fig. 4B). In NIH 3T3 cells cotransfected with either Rev-independent (Fig.

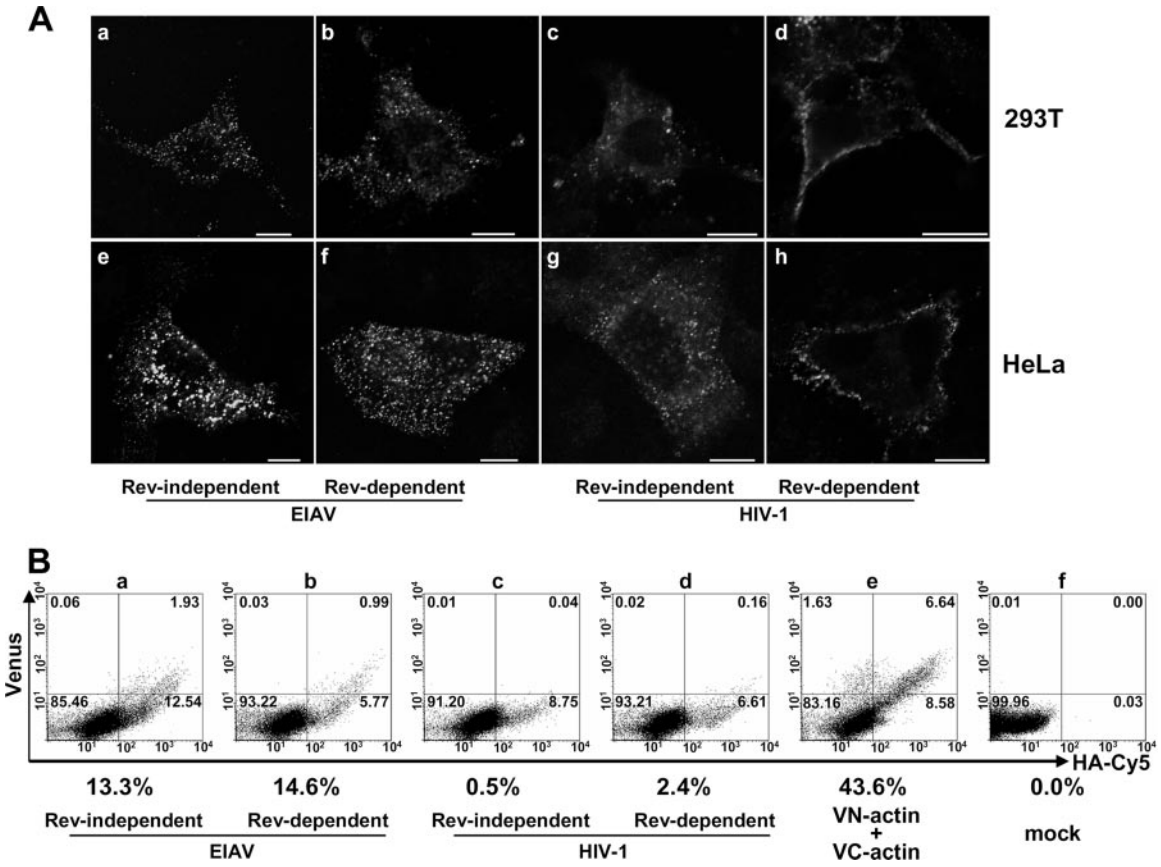

FIG. 3. BiFC analysis of EIAV and HIV-1 Gag assembly in human cells. (A) Visualization of Gag assembly by BiFC assay. 293T (panels a to d) and HeLa (panels e to h) cells grown on glass coverslips were transfected with Rev-independent EIAV-Gag-VN/Gag-VC (panels a and e), Rev-dependent EIAV-Gag-VN/Gag-VC (panels b and f), Rev-independent HIV-Gag-VN/Gag-VC (panels c and g), and Rev-dependent HIV-Gag-VN/Gag-VC (panels d and h) plasmid pairs using Lipofectamine 2000. At 16 h posttransfection, cells were fixed and imaged with a Leica TCS-SL confocal microscope. Bar, 10 μm. (B) Quantitative analysis by flow cytometry of BiFC signals in transient transfected HeLa cells described in panel A. At 16 h posttransfection, permeabilized cells were stained with mouse HA antibody and Cy5-conjugated goat anti-mouse IgG. A minimum of 30,000 gated live events were acquired and analyzed by both yellow and HA-Cy5 fluorescence. The percentage of HA and BiFC double-positive cells in total HA-positive cells was calculated and labeled below each quadrant plot.

4B, panel a) or Rev-dependent (Fig. 4B, panel b) EIAV Gag-VN/Gag-VC pairs, about 62% and 48% of HA-positive cells displayed positive BiFC signals, respectively. However, the assembly efficiency of Rev-independent (Fig. 4B, panel c) HIV-1 Gag observed in NIH 3T3 cells was roughly fivefold higher (49% versus 10%) than that of Rev-dependent HIV-1 Gag (Fig. 4B, panel d). Approximately 60% of HA-positive cells were BiFC positive in VN-actin/VC-actin-cotransfected NIH 3T3 cells (Fig. 4B, panel e), and no BiFC signal was detected in negative control rodent cells (Fig. 4B, panel f). These results indicate that the block of HIV-1 Gag assembly in NIH 3T3 cells with Rev-dependent Gag expression could be overcome by PRE-mediated RNA nuclear export. In marked contrast, both Rev-independent and Rev-dependent EIAV Gag could assemble efficiently in NIH 3T3 cells, indicating critical differences in EIAV and HIV-1 Gag assembly processes in rodent cells.

To confirm that the Gag-Gag-BiFC signals observed in cells transfected with various Gag-BiFC pairs represented functional Gag assembly, VLPs released from 293T (Fig. 5) or NIH 3T3 (data not shown) cells were visualized by confocal microscopy. Positive BiFC-labeled particles could be detected in supernatant pellets produced from 293T cells transfected with various Gag-VN/Gag-VC pairs, indicating that the Gag-Gag-BiFC complexes could be successfully incorporated into VLPs and that BiFC signals observed in cells represented functional assembly of Gag polyproteins.

Comparison of Rev-dependent and Rev-independent EIAV and HIV-1 Gag budding. Rev-dependent and Rev-independent EIAV and HIV-1 Gag budding efficiencies were also examined by Western blot analysis (Fig. 6). Four micrograms of total DNA was used to transfect one well of cells grown in six-well plates as described above for confocal microscopic and flow cytometric analysis. Cell lysates and pelleted VLPs produced from transfected 293T (Fig. 6A) or NIH 3T3 (Fig. 6) cells were analyzed by Western blotting at 48 h posttransfection. In human cells, the HIV-1 VLP budding efficiency of the Rev-independent HIV-1 Gag-VN/Gag-VC pair was roughly 10-fold lower than that of the Rev-dependent HIV-1 Gag-VN/Gag-VC pair (compare lane 3 with lanes 4 and 5 in Fig. 6A), consistent with the budding efficiency of singly transfected HIV-1 Gag-BiFC constructs

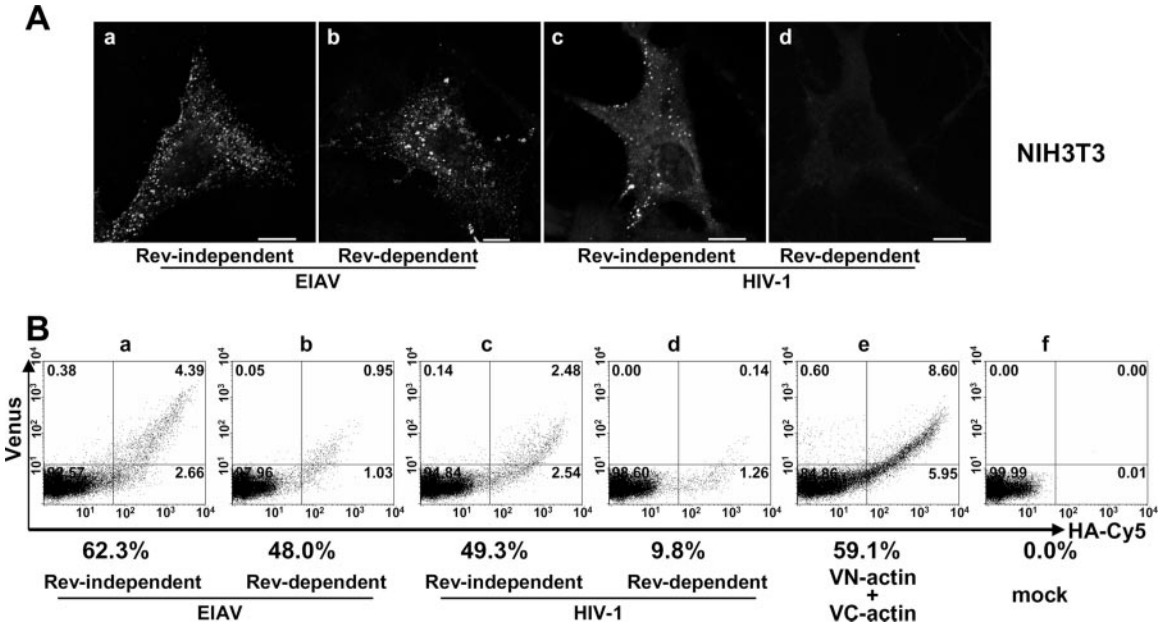

FIG. 4. BiFC analysis of EIAV and HIV-1 Gag assembly in NIH 3T3 cells. (A) Visualization of Gag assembly by BiFC assay. NIH 3T3 cells grown on glass coverslips were transfected with Rev-independent EIAV-Gag-VN/Gag-VC (panel a), Rev-dependent EIAV-Gag-VN/Gag-VC (panel b), Rev-independent HIV-Gag-VN/Gag-VC (panel c), and Rev-dependent HIV-Gag-VN/Gag-VC (panel d) plasmid pairs using Lipofectamine 2000. At 16 h posttransfection, cells were fixed and imaged with a Leica TCS-SL confocal microscope. Bar, 10 μm. (B) Quantitative analysis by flow cytometry of BiFC signals in transient transfected NIH 3T3 cells described in panel A. At 48 h posttransfection, cells were analyzed by flow cytometry as described in Fig. 3, except that rat HA antibody and Cy5-conjugated goat anti-rat IgG were used.

shown in Fig. 1B. Both Rev-independent (Fig. 6A, lane 1) and Rev-dependent (Fig. 6A, lane 2) EIAV Gag budded with an efficiency comparable that of Rev-dependent (Fig. 6A, lane 4) HIV-1 Gag in 293T cells.

In NIH 3T3 cells, both Rev-independent EIAV (Fig. 6A, lane 6) and HIV-1 (Fig. 6A, lane 8) Gag-BiFC constructs expressed Gag proteins and released VLPs at similar levels. However, the expression levels of Rev-dependent EIAV (Fig. 6A, lane 7) and HIV-1 (Fig. 6A, lane 9) Gag-BiFC constructs were relatively low in NIH 3T3 cells. These reduced Gag-BiFC construct expression levels correlated with greatly reduced VLP production by Rev-dependent EIAV Gag-BiFC (Fig. 6A, lane 7) and undetectable VLP production by Rev-dependent HIV-1 Gag-BiFC (Fig. 6A, lane 9).

To determine if the reduced VLP production by Rev-dependent EIAV or HIV-1 Gag in NIH 3T3 cells was the result of low Gag protein expression, cells were transfected with reduced amounts of Rev-independent EIAV (Fig. 6B) and HIV-1 (Fig. 6C) Gag-BiFC plasmids and serial dilution of VLPs and cell lysates from Rev-independent Gag-BiFC

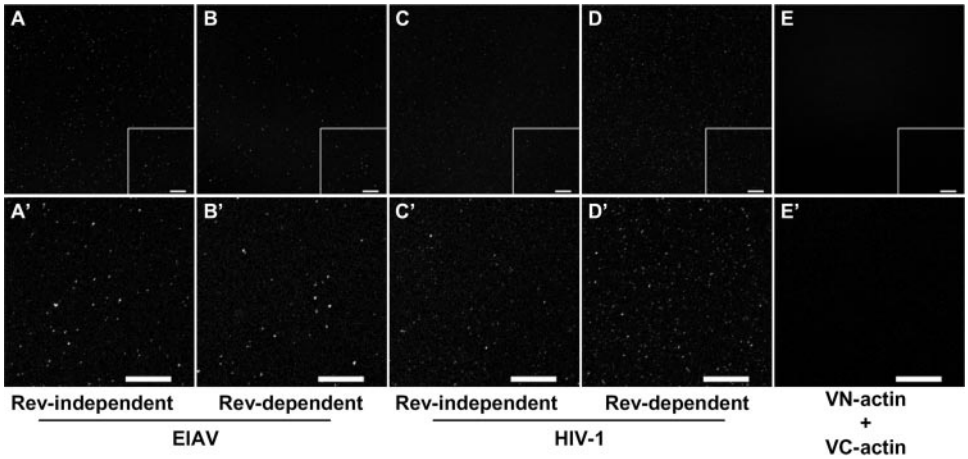

FIG. 5. Demonstration of BiFC Gag complexes in assembled VLPs. VLPs produced from 293T cells transfected with Rev-independent EIAV-Gag-VN/Gag-VC (A), Rev-dependent EIAV-Gag-VN/Gag-VC (B), Rev-independent HIV-Gag-VN/Gag-VC (C), Rev-dependent HIV-Gag-VN/Gag-VC (D), and VN-actin/VC-actin (E) plasmid pairs were immobilized on coverslips and fixed. Images were acquired on a Leica TCS-SL confocal microscope. Enlarged images of boxed areas in A to E are presented as A′ to E′. Bar, 10 μm.

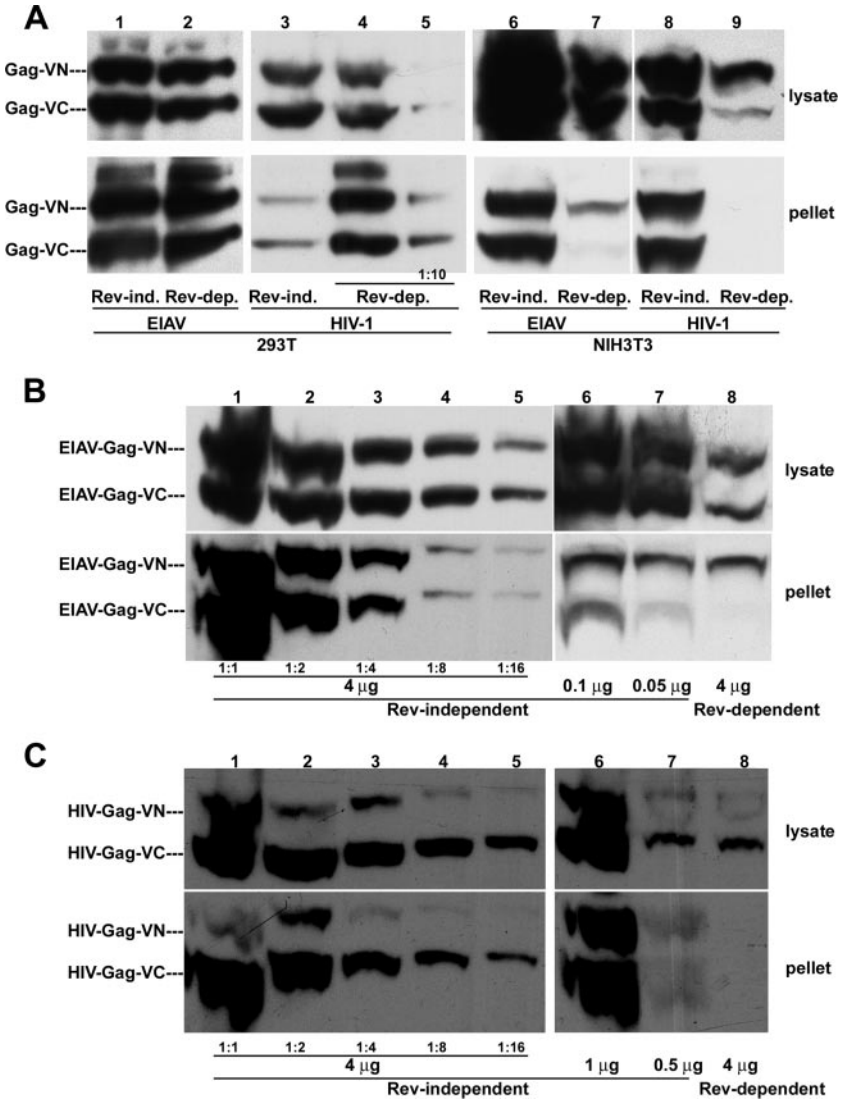

FIG. 6. Comparison of budding efficiencies of Rev-dependent and Rev-independent EIAV and HIV-1 Gag in human and rodent cells. (A) Expression and budding of cotransfected Gag-BiFC constructs. 293T (lanes 1 to 5) and NIH 3T3 (lanes 6 to 9) cells were cotransfected with Rev-independent EIAV-Gag-VN/Gag-VC (lanes 1 and 6), Rev-dependent EIAV-Gag-VN/Gag-VC (lanes 2 and 7), Rev-independent HIV-Gag-VN/Gag-VC (lanes 3 and 8), and Rev-dependent HIV-Gag-VN/Gag-VC (lanes 4, 5, and 9) plasmid pairs using Lipofectamine 2000. At 48 h posttransfection, cell lysates (upper panel) and VLPs (lower panel) were analyzed by immunoblotting using HA antibody. The tenfold diluted sample loaded on lane 4 was loaded on lane 5. (B) Comparison of budding efficiencies of Rev-independent and Rev-dependent EIAV in NIH 3T3 cells. The indicated amounts of Rev-independent and Rev-dependent EIAV and Gag-BiFC plasmid pairs were used for transfection in NIH 3T3 cells. At 48 h posttransfection, cell lysates (upper panel) and VLPs (lower panel) were analyzed by immunoblotting using HA antibody. Serial dilutions of Rev-independent samples were analyzed in parallel. (C) Comparison of budding efficiencies of Rev-independent and Rev-dependent HIV-1 in NIH 3T3 cells as described in panel B, except that HIV-1 Gag-BiFC plasmid pairs were used for transfection.

plasmid-transfected cells were used to compare Rev-dependent and Rev-independent Gag budding at equally low protein expression levels. Similar levels of VLPs were released from NIH 3T3 cells expressing comparable amounts of Rev-dependent (Fig. 6B, lane 8) and Rev-independent (Fig. 6B, lanes 5 and 7) EIAV Gag-BiFC constructs. However, in NIH 3T3 cells expressing comparable levels of Rev-independent (Fig. 6C, lanes 5 and 7) and Rev-dependent (Fig. 6C, lane 8) HIV-1 Gag-BiFC constructs, Gag-VN and Gag-VC were released only in cells expressing the Rev-independent constructs.

DISCUSSION

In the current study, we utilized the newly developed BiFC assay to study EIAV and HIV-1 Gag assembly and budding in human and mouse cell types, both qualitatively and quantitatively. Using the BiFC method, which enables highly specific and sensitive detection of in vivo protein-protein interactions (19, 22, 34), we were able to correlate Gag assembly efficiency with VLP budding efficiency, as well as to confirm the incorporation of Gag-Gag BiFC complexes into VLPs, further validating this technique as a tool to study functional viral assem-

bly. The BiFC studies described here for the first time compare in one study the Gag assembly sites of an animal lentivirus with HIV-1, directly testing the assumption that all lentiviruses assemble via identical pathways in the same target cell. Thus, the results of these comparative studies reveal novel insights into fundamental properties of lentivirus assembly mechanisms and identify new systems in which to elucidate specific virus-cell interactions that can facilitate or inhibit assembly in human or rodent cells.

EIAV and HIV-1 Gag use distinct trafficking routes during viral assembly/budding. Currently, the sites of retrovirus assembly and budding are vigorously debated topics. It has been generally assumed that lentiviral assembly and budding pathways follow the assembly pathway defined for type-C oncoviruses, such as murine or avian leukemia viruses, in which Gag polyproteins assemble and bud at specific plasma membrane sites to form viral particles. Although a large number of studies have been performed to characterize HIV-1 assembly and budding in various cell types using diverse techniques, assembly and budding mechanisms of other lentiviruses have not been well characterized. Data from our lab and others have previously indicated that EIAV and HIV-1 may use related but distinct assembly pathways and that these differences could be exploited to define critical virus-cell interactions that mediate Gag trafficking and assembly (7, 38, 41, 44). For example, EIAV is unique from other retroviruses in that its assembly and budding is insensitive to proteasome inhibitor treatments that deplete intracellular free ubiquitin, whereas budding of HIV-1 and other retroviruses is inhibited by the same proteasome inhibitor treatments (38, 39). Like other retroviruses, EIAV assembly and budding are suppressed by dominant-negative VPS4A (28, 44, 51) but are insensitive to the expression of carboxy-terminal fragments of TSG101 that inhibit PTAP and PPPY L-domain-mediated Gag assembly and budding (44). EIAV Gag utilizes a unique L domain, a YPDL motif, that recruits host VPS protein Alix/AIP1 (27, 47, 52) and adaptor protein complex AP-2 (41), both of which are required for efficient EIAV budding (7). Therefore, although EIAV Gag assembly and budding pathways converge with other retroviral assembly and budding pathways at the final step by entry into ESCRTs endosomal sorting network, these differences suggest that EIAV Gag may use a unique portal of entry to the endosomal sorting network and upstream trafficking pathway.

In the current study, we characterized EIAV Gag assembly in various cell lines and compared EIAV Gag and HIV-1 Gag assembly and budding by the BiFC assay. Distinct assembly sites for EIAV Gag (intracellular) and HIV-1 Gag (cell surface) were revealed in human cells where both Gag species budded efficiently. In rodent cells, compared to the efficient assembly and budding of EIAV Gag, HIV-1 Gag neither assembled nor budded. It is important to note that there was a close correlation between the levels of Gag multimerization detected by BiFC in various cell types and the levels of VLP production from the respective cell types. Taken together, these data indicate distinct intracellular trafficking of EIAV and HIV-1 Gag in the same target human or rodent cells. Interestingly, while the intracellular assembly pattern of EIAV Gag in fibroblastic cells is distinct from that of HIV-1 in these cells (10, 29, 31, 36), it is reminiscent of HIV-1 Gag intracellular assembly observed in human macrophages (40, 42). Recent studies have suggested that HIV-1 in human macrophages may assemble and bud from invaginated membrane domains that resemble endosomal structures but are contiguous with the plasma membrane (11, 53). Earlier reports demonstrated a failure to release HIV-1 Gag that was targeted to endosomes either by inducing phosphatidylinositol 4,5-bisphosphate synthesis on endosome membranes (35) or by replacing the HIV-1 Gag membrane-targeting signal with phosphatidylinositol 3-phosphate binding domains (21), supporting the model that the plasma membrane is the productive budding site for HIV-1 in human cells. In contrast to HIV-1 Gag, intracellularly assembled EIAV Gag budded efficiently from both human and rodent cells, the latter being unable to support HIV-1 Gag assembly and budding. Identification of the intracellular sites where EIAV Gag assembles and the cellular factors that mediate EIAV release in various cell types will enable us to determine both common and distinct paradigms of retrovirus assembly and budding.

The intracellular assembly pattern of EIAV Gag was also observed in equine fibroblasts. It remains to be determined if these patterns are also observed in equine macrophages, the natural target cell for primary isolates of EIAV. However, it is important to note that the EIAVuk proviral strain used in this study is cell adapted via changes in its long terminal repeat sequences (9) such that it can productively infect cultured equine fibroblastic cells and is able to produce fully infectious virus particles from various transfected human cell lines. In this regard, equine and human fibroblastic cell lines have been used extensively to study EIAV assembly and budding (6, 7, 25, 38, 44). With the development of the BiFC assay to study EIAV Gag assembly, it should now be possible to extend these types of studies to define EIAV assembly in its natural target cells.

mRNA nuclear export pathways influence Gag assembly and budding sites. Although no obvious changes in EIAV Gag assembly and budding were observed after altering Rev-mediated mRNA nuclear export to hepatitis B virus PRE-mediated mRNA nuclear export, marked changes in HIV-1 Gag assembly location and assembly/budding efficiency were observed. These differences included relocation of HIV-1 Gag assembly sites from the plasma membrane to intracellular sites in human cells and rescue of HIV-1 Gag assembly and budding in NIH 3T3 cells. Rev-dependent HIV-1 Gag was reported to form condensed, electron-dense structures (26), presumably aggregates of Gag polyproteins, and to display a diffuse distribution pattern in NIH 3T3 cells, indicating an assembly deficiency (4, 49). The current results showed that Rev-dependent HIV-1 Gag did not form BiFC complexes in mouse cells, indicating either that the reported abnormal aggregation of HIV-1 Gag in NIH 3T3 cells is extremely inefficient or that Gag polyproteins in the aggregates are not associated in an arrangement that favors BiFC complex formation. Alternative HIV-1 Gag assembly and budding pathways were previously reported in different cells types (33, 36), as well as in nonlymphoid cell lines expressing HLA-DR epigenetically (14). However, the mechanisms that drive the selection of alternative assembly and budding pathways are largely unknown. Consistent with a recent study (49), the current data indicate that distinct mRNA export pathways regulate HIV-1 Gag assembly and budding pathways.

RNA export pathways could modulate the cytosolic fate or function of Gag polyproteins at three levels. (i) Retroviral genomic RNA (gRNA) is associated with proteins to form ribonucleoprotein particles (RNP), and RNP components might regulate gRNA trafficking and subsequent Gag assembly (8). Indeed, one such component (hnRNP A2) has previously been reported to regulate HIV-1 gRNA trafficking and virus production (24). (ii) Retrovirus Gag assembly is a stepwise, energy-dependent process that requires chaperone proteins (13, 16, 18, 55). Therefore, differences in Gag synthesis sites as a consequence of different RNA nuclear export pathways might lead to exposure of Gag to different cellular factors. The failure to recruit necessary chaperones could result in defective assembly and explain the inefficient assembly of Rev-dependent HIV-1 Gag in NIH 3T3 cells. (iii) Retroviral Gag trafficking to budding sites also depends on other cellular factors including motor proteins and membrane trafficking regulators (6, 7, 10, 12, 23, 29, 43, 50). Mislocalization of Gag polyproteins might prevent recruitment of partners required for Gag transport, even if Gag assembly per se is competent. The latter might explain the low budding efficiency of intracellularly assembled HIV-1 Gag in human cells.

Elucidating the mechanisms by which Rev-dependent HIV-1 Gag assembly is blocked in rodent cells and by which Rev-independent Gag overcomes this block could help to develop small animal models of HIV-1 replication and pathogenesis. Further studies are needed to examine how RNA export regulates HIV-1 Gag trafficking and assembly, to define what factors regulate the release of intracellular versus plasma membrane assembled HIV-1 in human cells, and to identify the machinery that enables efficient intracellular assembly/budding of EIAV Gag. Based on the current studies of EIAV and HIV-1 Gag assembly, we propose that additional comparisons of animal and human lentivirus assembly pathways can accelerate these mechanistic studies of lentivirus Gag assembly and budding processes and increase the potential to develop novel antiviral therapies targeting Gag assembly and budding.

ACKNOWLEDGMENTS

We express our appreciation to Atsushi Miyawaki and Eric Freed for generous gifts of plasmids used in these studies and to Eric Freed, Feng Li, and Ted Ross for helpful discussions and critical readings of the manuscript.

This research was supported by NIH grant R01 CA49296 (R.C.M.).

REFERENCES

1. **Bieniasz, P. D., and B. R. Cullen.** 2000. Multiple blocks to human immunodeficiency virus type 1 replication in rodent cells. J. Virol. **74:**9868–9877.
2. **Blom, J., C. Nielsen, and J. M. Rhodes.** 1993. An ultrastructural study of HIV-infected human dendritic cells and monocytes/macrophages. APMIS **101:**672–680.
3. **Boyko, V., M. Leavitt, R. Gorelick, W. Fu, O. Nikolaitchik, V. K. Pathak, K. Nagashima, and W. S. Hu.** 2006. Coassembly and complementation of Gag proteins from HIV-1 and HIV-2, two distinct human pathogens. Mol. Cell **23:**281–287.
4. **Chen, B. K., I. Rousso, S. Shim, and P. S. Kim.** 2001. Efficient assembly of an HIV-1/MLV Gag-chimeric virus in murine cells. Proc. Natl. Acad. Sci. USA **98:**15239–15244.
5. **Chen, C., F. Li, and R. C. Montelaro.** 2001. Functional roles of equine infectious anemia virus Gag p9 in viral budding and infection. J. Virol. **75:**9762–9770.
6. **Chen, C., J. Jin, M. Rubin, L. Huang, T. Sturgeon, K. M. Weixel, D. B. Stolz, S. C. Watkins, J. R. Bamburg, O. A. Weisz, and R. C. Montelaro.** 2007. Association of Gag multimers with filamentous actin during equine infectious anemia virus assembly. Curr. HIV Res. **5:**315–323.
7. **Chen, C., O. Vincent, J. Jin, O. A. Weisz, and R. C. Montelaro.** 2005. Functions of early (AP-2) and late (AIP1/ALIX) endocytic proteins in equine infectious anemia virus budding. J. Biol. Chem. **280:**40474–40480.
8. **Cochrane, A., M. McNally, and A. Mouland.** 2006. The retrovirus RNA trafficking granule: from birth to maturity. Retrovirology **3:**18.
9. **Cook, R. F., C. Leroux, S. J. Cook, S. L. Berger, D. L. Lichtenstein, N. N. Ghabrial, R. C. Montelaro, and C. J. Issel.** 1998. Development and characterization of an in vivo pathogenic molecular clone of equine infectious anemia virus. J. Virol. **72:**1383–1393.
10. **Demirov, D. G., and E. O. Freed.** 2004. Retrovirus budding. Virus Res. **106:**87–102.
11. **Deneka, M., A. Pelchen-Matthews, R. Byland, E. Ruiz-Mateos, and M. Marsh.** 2007. In macrophages, HIV-1 assembles into an intracellular plasma membrane domain containing the tetraspanins CD81, CD9, and CD53. J. Cell Biol. **177:**329–341.
12. **Dong, X., H. Li, A. Derdowski, L. Ding, A. Burnett, X. Chen, T. R. Peters, T. S. Dermody, E. Woodruff, J. J. Wang, and P. Spearman.** 2005. AP-3 directs the intracellular trafficking of HIV-1 Gag and plays a key role in particle assembly. Cell **120:**663–674.
13. **Dooher, J. E., and J. R. Lingappa.** 2004. Conservation of a stepwise, energy-sensitive pathway involving HP68 for assembly of primate lentivirus capsids in cells. J. Virol. **78:**1645–1656.
14. **Finzi, A., A. Brunet, Y. Xiao, J. Thibodeau, and E. A. Cohen.** 2006. Major histocompatibility complex class II molecules promote human immunodeficiency virus type 1 assembly and budding to late endosomal/multivesicular body compartments. J. Virol. **80:**9789–9797.
15. **Freed, E. O., and M. A. Martin.** 1995. Virion incorporation of envelope glycoproteins with long but not short cytoplasmic tails is blocked by specific, single amino acid substitutions in the human immunodeficiency virus type 1 matrix. J. Virol. **69:**1984–1989.
16. **Gurer, C., A. Cimarelli, and J. Luban.** 2002. Specific incorporation of heat shock protein 70 family members into primate lentiviral virions. J. Virol. **76:**4666–4670.
17. **Hermida-Matsumoto, L., and M. D. Resh.** 2000. Localization of human immunodeficiency virus type 1 Gag and Env at the plasma membrane by confocal imaging. J. Virol. **74:**8670–8679.
18. **Hong, S., G. Choi, S. Park, A. S. Chung, E. Hunter, and S. S. Rhee.** 2001. Type D retrovirus Gag polyprotein interacts with the cytosolic chaperonin TRiC. J. Virol. **75:**2526–2534.
19. **Hu, C. D., Y. Chinenov, and T. K. Kerppola.** 2002. Visualization of interactions among bZIP and Rel family proteins in living cells using bimolecular fluorescence complementation. Mol. Cell **9:**789–798.
20. **Hu, C. D., and T. K. Kerppola.** 2003. Simultaneous visualization of multiple protein interactions in living cells using multicolor fluorescence complementation analysis. Nat. Biotechnol. **21:**539–545.
21. **Jouvenet, N., S. J. D. Neil, C. Bess, M. C. Johnson, C. A. Virgen, S. M. Simon, and P. D. Bieniasz.** 2006. Plasma membrane is the site of productive HIV-1 particle assembly. PLoS Biol. **4:**e435.
22. **Kerppola, T. K.** 2006. Visualization of molecular interactions by fluorescence complementation. Nat. Rev. Mol. Cell Biol. **7:**449–456.
23. **Leung, J., A. Yueh, F. J. Appah, B. Yuan, K. de los Santos, and S. Goff.** 2006. Interaction of Moloney murine leukemia virus matrix protein with IQGAP. EMBO J. **25:**2155–2166.
24. **Levesque, K., M. Halvorsen, L. Abrahamyan, L. Chatel-Chaix, V. Poupon, H. Gordon, L. DesGroseillers, A. Gatignol, and A. J. Mouland.** 2006. Trafficking of HIV-1 RNA is mediated by heterogeneous nuclear ribonucleoprotein A2 expression and impacts on viral assembly. Traffic **7:**1177–1193.
25. **Li, F., C. Chen, B. A. Puffer, and R. C. Montelaro.** 2002. Functional replacement and positional dependence of homologous and heterologous L domains in equine infectious anemia virus replication. J. Virol. **76:**1569–1577.
26. **Mariani, R., G. Rutter, M. E. Harris, T. J. Hope, H. G. Krausslich, and N. R. Landau.** 2000. A block to human immunodeficiency virus type 1 assembly in murine cells. J. Virol. **74:**3859–3870.
27. **Martin-Serrano, J., A. Yarovoy, D. Perez-Caballero, and P. D. Bieniasz.** 2003. Divergent retroviral late-budding domains recruit vacuolar protein sorting factors by using alternative adaptor proteins. Proc. Natl. Acad. Sci. USA **100:**12414–12419.
28. **Martin-Serrano, J., T. Zang, and P. D. Bieniasz.** 2003. Role of ESCRT-I in retroviral budding. J. Virol. **77:**4794–4804.
29. **Morita, E., and W. I. Sundquist.** 2004. Retrovirus budding. Annu. Rev. Cell Dev. Biol. **20:**395–425.
30. **Nasioulas, G., S. H. Hughes, B. K. Felber, and J. M. Whitcomb.** 1995. Production of avian leukosis virus particles in mammalian cells can be mediated by the interaction of the human immunodeficiency virus protein Rev and the Rev-responsive element. Proc. Natl. Acad. Sci. USA **92:**11940–11944.
31. **Neil, S. J. D., S. W. Eastman, N. Jouvenet, and P. D. Bieniasz.** 2006. HIV-1 Vpu promotes release and prevents endocytosis of nascent retrovirus particles from the plasma membrane. PLoS Pathogens **2:**e39.
32. **Nguyen, D. G., A. Booth, S. J. Gould, and J. E. K. Hildreth.** 2003. Evidence that HIV budding in primary macrophages occurs through the exosome release pathway. J. Biol. Chem. **278:**52347–52354.

33. **Nydegger, S., M. Foti, A. Derdowski, P. Spearman, and M. Thali.** 2003. HIV-1 egress is gated through late endosomal membranes. Traffic **4:**902–910.
34. **Nyfeler, B., S. W. Michnick, and H. P. Hauri.** 2005. Capturing protein interactions in the secretory pathway of living cells. Proc. Natl. Acad. Sci. USA **102:**6350–6355.
35. **Ono, A., S. D. Ablan, S. J. Lockett, K. Nagashima, and E. O. Freed.** 2004. Phosphatidylinositol (4,5) bisphosphate regulates HIV-1 Gag targeting to the plasma membrane. Proc. Natl. Acad. Sci. USA **101:**14889–14894.
36. **Ono, A., and E. O. Freed.** 2004. Cell-type-dependent targeting of human immunodeficiency virus type 1 assembly to the plasma membrane and the multivesicular body. J. Virol. **78:**1552–1563.
37. **Otero, G. C., M. E. Harris, J. E. Donello, and T. J. Hope.** 1998. Leptomycin B inhibits equine infectious anemia virus Rev and feline immunodeficiency virus Rev function but not the function of the hepatitis B virus posttranscriptional regulatory element. J. Virol. **72:**7593–7597.
38. **Patnaik, A., V. Chau, F. Li, R. C. Montelaro, and J. W. Wills.** 2002. Budding of equine infectious anemia virus is insensitive to proteasome inhibitors. J. Virol. **76:**2641–2647.
39. **Patnaik, A., V. Chau, and J. W. Wills.** 2000. Ubiquitin is part of the retrovirus budding machinery. Proc. Natl. Acad. Sci. USA **97:**13069–13074.
40. **Pelchen-Matthews, A., B. Kramer, and M. Marsh.** 2003. Infectious HIV-1 assembles in late endosomes in primary macrophages. J. Cell Biol. **162:**443–455.
41. **Puffer, B. A., S. C. Watkins, and R. C. Montelaro.** 1998. Equine infectious anemia virus Gag polyprotein late domain specifically recruits cellular AP-2 adapter protein complexes during virion assembly. J. Virol. **72:**10218–10221.
42. **Raposo, G., M. Moore, D. Innes, R. Leijendekker, A. Leigh-Brown, P. Benaroch, and H. Geuze.** 2002. Human macrophages accumulate HIV-1 particles in MHC II compartments. Traffic **3:**718–729.
43. **Sasaki, H., M. Nakamura, T. Ohno, Y. Matsuda, Y. Yuda, and Y. Nonomura.** 1995. Myosin-actin interaction plays an important role in human immunodeficiency virus type 1 release from host cells. Proc. Natl. Acad. Sci. USA **92:**2026–2030.
44. **Shehu-Xhilaga, M., S. Ablan, D. G. Demirov, C. Chen, R. C. Montelaro, and E. O. Freed.** 2004. Late domain-dependent inhibition of equine infectious anemia virus budding. J. Virol. **78:**724–732.
45. **Sherer, N. M., M. J. Lehmann, L. F. Jimenez-Soto, A. Ingmundson, S. M. Horner, G. Cicchetti, P. G. Allen, M. Pypaert, J. M. Cunningham, and W. Mothes.** 2003. Visualization of retroviral replication in living cells reveals budding into multivesicular bodies. Traffic **4:**785–801.
46. **Shyu, Y. J., H. Liu, X. Deng, and C. D. Hu.** 2006. Identification of new fluorescent protein fragments for bimolecular fluorescence complementation analysis under physiological conditions. BioTechniques **40:**61–66.
47. **Strack, B., A. Calistri, S. Craig, E. Popova, and H. G. Gottlinger.** 2003. AIP1/ALIX is a binding partner for HIV-1 p6 and EIAV p9 functioning in virus budding. Cell **114:**689–699.
48. **Swanson, C. M., and M. H. Malim.** 2006. Retrovirus RNA trafficking: from chromatin to invasive genomes. Traffic **7:**1440–1450.
49. **Swanson, C. M., B. A. Puffer, K. M. Ahmad, R. W. Doms, and M. H. Malim.** 2004. Retroviral mRNA nuclear export elements regulate protein function and virion assembly. EMBO J. **23:**2632–2640.
50. **Tang, Y., U. Winkler, E. O. Freed, T. A. Torrey, W. Kim, H. Li, S. P. Goff, and H. C. Morse III.** 1999. Cellular motor protein KIF-4 associates with retroviral Gag. J. Virol. **73:**10508–10513.
51. **Tanzi, G. O., A. J. Piefer, and P. Bates.** 2003. Equine infectious anemia virus utilizes host vesicular protein sorting machinery during particle release. J. Virol. **77:**8440–8447.
52. **von Schwedler, U. K., M. Stuchell, B. Muller, D. M. Ward, H. Y. Chung, E. Morita, H. E. Wang, T. Davis, G. P. He, D. M. Cimbora, A. Scott, H. G. Krausslich, J. Kaplan, S. G. Morham, and W. I. Sundquist.** 2003. The protein network of HIV budding. Cell **114:**701–713.
53. **Welsch, S., O. T. Keppler, A. Habermann, I. Allespach, J. Krijnse-Locker, and H. G. Krausslich.** 2007. HIV-1 buds predominantly at the plasma membrane of primary human macrophages. PLoS Pathogens **3:**e36.
54. **Zang, W. Q., and T. S. Benedict Yen.** 1999. Distinct export pathway utilized by the hepatitis B virus posttranscriptional regulatory element. Virology **259:**299–304.
55. **Zimmerman, C., K. C. Klein, P. K. Kiser, A. R. Singh, B. L. Firestein, S. C. Riba, and J. R. Lingappa.** 2002. Identification of a host protein essential for assembly of immature HIV-1 capsids. Nature **415:**88–92.